

Comparison of Tidal and Wind Contributions to Lagrangian Trajectories in the Southwestern Yellow Sea

Wang, Bin

Department of Earth System Science and Technology, Kyushu University

Hirose, Naoki

Research Institute for Applied Mechanics, Kyushu University

Moon, Jae-Hong

Jet Propulsion Laboratory, California Institute of Technology

Yuan, Dongliang

Key Laboratory of Ocean Circulation and Waves, Chinese Academy of Sciences | Institute of Oceanology, Chinese Academy of Sciences

<https://doi.org/10.15017/27135>

出版情報：九州大学応用力学研究所所報. 143, pp.43-48, 2012-09. Research Institute for Applied Mechanics, Kyushu University

バージョン：

権利関係：

Comparison of Tidal and Wind Contributions to Lagrangian Trajectories in the Southwestern Yellow Sea

Bin WANG^{*1}, Naoki HIROSE^{*1, *2}, Jae-Hong MOON^{*3} and Dongliang YUAN^{*4, *5}

E-mail of corresponding author: wangbin@riam.kyushu-u.ac.jp

(Received July 31, 2012)

Abstract

The Lagrangian trajectories in the southwestern Yellow Sea in response to tidal and wind forces are investigated using a high-resolution circulation model. The simulated tidal harmonic constants agree with the observations and existing studies well. The numerical experiment reproduces the long-range southeastward Eulerian tidal residual current over the sloping bottom around Yangtze Bank as shown in previous studies. However, the artificial drifters deployed at the northeast flank of Yangtze Bank in the simulation move northward against this strong southeastward Eulerian tidal residual current rather than following it. The result suggests that the influence of tidal residual currents on Lagrangian trajectories is weaker than that of southerly wind. Thus, the Lagrangian trajectories are dominated by wind driven currents in the southwestern Yellow Sea. The result is consistent with the northeastward movement of ARGOS surface drifters released in the southwestern Yellow Sea in the summer of 2009. Further analyses suggest that the quadratic bottom friction scheme is the crucial factor for the weaker influence of the tidal residual currents on Lagrangian trajectories in the southwestern Yellow Sea. This study demonstrates that the movement directions of Lagrangian trajectory and Eulerian velocity are different at shallow coastal regions due to nonlinearity of the bottom friction.

Key words: Eulerian velocity, Lagrangian velocity, Yellow Sea, Tidal residual current, Lagrangian drifter, Bottom friction scheme

1. Introduction

The Yellow Sea is a semi-enclosed embayment located between China mainland and the Korean Peninsula. The bottom of the southwestern Yellow Sea is very varied, with a quite shallow water depth, especially for Yangtze Bank where the water depth is generally less than 20 m (Fig 1). The basin geometry, varied topography and shallow water depth cause that the circulations and tides in this area are extremely complex and difficult to model and predict. Furthermore, due to the limited direct current measurements, until now, the understanding of the circulation in the

southwestern Yellow Sea is still highly primitive.

The tides and tidal currents in the East China Sea and Yellow Sea, have been well-known to investigators by the field observation data (Ogura, 1933; Nishida, 1980; Larsen et al., 1985; Fang, 1986), the satellite altimetric sea levels data (Yanagi et al., 1997) and the sorts of numerical models (An, 1977; Shen, 1980; Choi, 1980, 1984, 1990; Yanagi and Inoue, 1994; Zhao et al., 1994; Ye and Mei, 1995; Kang et al., 1998; Kang et al., 2002; Moon, 2009). According to the existing results, the Eulerian residual circulation formed a basin scale cyclonic in the Yellow Sea, while, it flowed northward along Subei coast as a part of an anticyclonic gyre. The researchers suggested that the large tidal amplitudes over the sharply sloping bottom around Yangtze Bank, where between the basin scale cyclonic circulation and anticyclonic gyre, produced strong southeastward residual currents. Particularly, as a result of the weak and less persistent winds and regional surface heating, the strong thermal stratification in summer led to a signally sub-surface intensification of this southeastward residual current (Lee and Beardsley, 1999), which could

¹ Department of Earth System Science and Technology, Kyushu University

² Research Institute for Applied Mechanics, Kyushu University

³ Jet Propulsion Laboratory, California Institute of Technology

⁴ Key Laboratory of Ocean Circulation and Wave, Chinese Academy of Sciences

⁵ Institute of Oceanology, Chinese Academy of Sciences

play an important role in the regional circulation. The conceptual models (Liu, 1986; Hu *et al.*, 1991, Hu, 1994), the drifter tracking observation (Beardsley *et al.*, 1992) and the numerical studies (Yanagi and Takahashi, 1993; Takahashi and Yanagi, 1995; Tang *et al.*, 2000; Xu *et al.*, 2002) revealed a cyclonic baroclinic frontal circulation associated with the strong thermal fronts in the central part of the Yellow Sea where roughly along the 40-50 m isobaths. The southeastward Eulerian tidal residual current was considered to strengthen the basin scale cyclonic circulation in the central part of the Yellow Sea in summer time (Xia *et al.*, 2006).

Recently, Yuan *et al.* (2008) discovered that the Subei coast current actually flowed northward in summer time in response to the southerly wind forcing. This northward flow was confirmed by the satellite track of the algal patches movements during the green tide event (*Ulva Prolifera* bloom) offshore Qingdao in the summer season of 2008 (Hu and He, 2008; Qiao *et al.*, 2008; Hu *et al.*, 2010). Furthermore, the trajectories of ARGOS surface drifters released in the southwestern Yellow Sea in the summer season of 2009 confirmed this northward Subei coast current (Li, 2010). Instead of following the southeastward Eulerian tidal residual current, the ARGOS surface drifters flowed northward through it. Thus, the effect of the tidal residual currents on Lagrangian behavior in the southwestern Yellow Sea

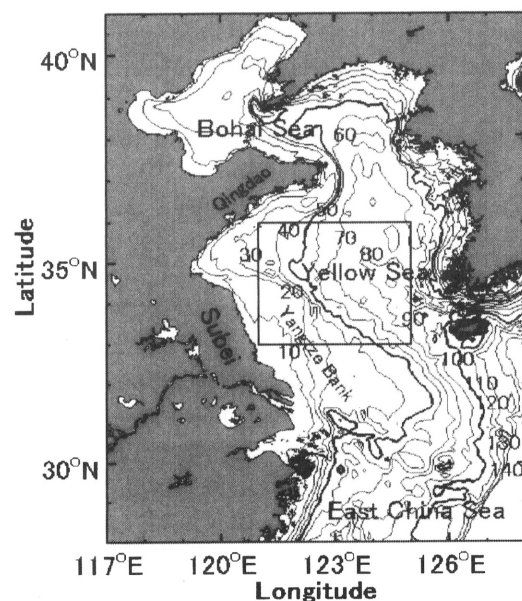


Fig 1. Model domain and topography; the box shows the area of interesting (in meter, the contour interval is 10 m).

caused a serious concern.

In this study, the influence of the tidal residual currents on Lagrangian trajectories in the southwestern Yellow Sea is investigated using a high-resolution

circulation model of the southwestern Yellow Sea with and without wind forcing.

2. Data and Model

The Princeton Ocean Model is applied (POM2k) to study the influence of the tidal residual currents on Lagrangian trajectories in the southwestern Yellow Sea. The model covers the domain of East China Sea (28°N-41°N, 117°E-128°E), with a horizontal resolution of $1/12^\circ \times 1/12^\circ$ and 16 levels in the vertical direction (Fig 1). The sigma coordinate are 0.000, -0.003, -0.006, -0.013, -0.025, -0.050, -0.100, -0.200, -0.300, -0.400, -0.500, -0.600, -0.700, -0.800, -0.900, -1.00, respectively, from surface to bottom. The topography is averaged from 12×12 depth data of the Coastal and Ocean Dynamics Studies Laboratory of Sungkyunkwan University (Choi *et al.*, 2002). Two modifications, setting the maximum water depth to be 140 m and the minimum water depth to be 1 m, are made on the original topography data to relax the CFL condition and to reduce possible error in the finite difference of the baroclinic pressure gradient over steep topography with a vertical sigma coordinate grid (Haney, 1991; Chen *et al.*, 1995a, b).

M_2 , S_2 , K_1 and O_1 tidal forcing are considered on the open boundary by using a fixed radiation condition for the depth-averaged velocity. The tidal amplitudes and phases come from the global $0.25^\circ \times 0.25^\circ$ TPX0.6 tide model (Gary *et al.*, 1994). The tidal forcing is ramped up to the full amplitude within the first two tidal periods to minimize starting transients. The reanalyze $2.5^\circ \times 2.5^\circ$ NCEP climatological wind stress fields are interpolated to force the model from May to June (~ 0.01 N/m²). The initial and boundary conditions are determined from a $1/4^\circ$ Western North Pacific Ocean Model (Hirose, 2011). The sea surface temperature and salinity are relaxed to the climatological ones.

Several experiments based on the numerical model are shown in Table 1. ExpQ.T is conducted only using the tidal forcing whereas ExpQ.W_c is only using climatological wind forcing. The third experiment called ExpQ.W_cT is designed with respect to both tidal and climatological wind forcing. In these three experiments, the bottom friction term given by the nonlinear quadratic parameterization as following:

$$\vec{F}_Q = -C_D |\vec{u}| \vec{u} \quad (1)$$

where \vec{u} is the near bottom velocity vector. The drag coefficient C_D is 0.001 in the Bohai Sea, north of the line between (37.80°N, 120.93°E) and (39.05°N, 121.96°E),

while it is 0.0016 in the other areas (Wan et al., 1998). The comparison of these three numerical experimental results will show the primary driving force of Lagrangian currents in the southwestern Yellow Sea. ExpL.T, ExpL.W_c and ExpL.W_cT are same conditions with ExpQ.T, ExpQ.W_c and ExpQ.W_cT, respectively, except that the former three cases adopting the linear Ekman bottom friction scheme presented as formula (2).

$$\vec{F}_E = -\Gamma_E \vec{u} \quad (2)$$

After some sensitivity experiments to match the non-linear cases, we chose the linear drag coefficients Γ_E as 0.0005 and 0.0008 in the Bohai Sea and the other areas, respectively. These three experiments will declare the dynamics of these Lagrangian phenomena.

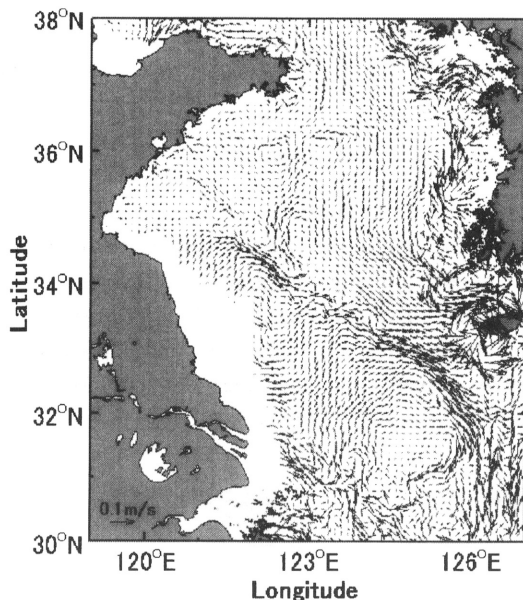


Fig 2. The simulated circulation at 15 m depth during June in ExpQ.W_cT

The Lagrangian behaviors of current in the southwestern Yellow Sea are studied by the trajectories of the artificial drifters, which are deemed as the Lagrangian tracers. The trajectories are calculated by the forth-order Runge-Kutta scheme. The positions of the drifters are calculated every 2 hours after model running 15 days in each experiment. A hundred artificial drifters are released at 15 m depth along the 33.80°N section in the southwestern Yellow Sea.

3. Results

3.1 Eulerian behavior

To verify the model results, harmonic constants are obtained by using harmonic analysis. The co-tidal charts of the M₂, S₂, K₁ and O₁ tides and depth-averaged Eulerian tidal residual current generate from the model are similar with existing studies (not shown here). Therefore, based on this model results, we obtain the circulation field at the depth of 15 m in June with regard to both tidal forcing and wind forcing (ExpQ.W_cT).

As displayed in Fig 2, the 15 m depth circulation in June denotes that a cyclonic circulation encompasses the entire deep basin. Along the Korean coast, it is a strong northward jet flow; on the contrary, it flows southward in the west and central parts of the Yellow Sea but much broader and weaker. Particularly, along the Subei coast, the northward current is much enhanced by tidally rectified. With the southeastward current over the sloping bottom around Yangtze Bank, an anticyclonic gyre is formed in the regional area against the western limb of the cyclonic current. This result is similar with the model result of Naimie et al. (2001) and the analysis of observation in Liu (2006). Furthermore, the horizontal temperature distribution at 30 m depth is illustrated in Fig 3a, which basically agrees with the result of Hirose (2011) that is shown in Fig 3b. To sum up, the model reproduced tides, tidal currents and circulation in the southwestern Yellow Sea successfully.

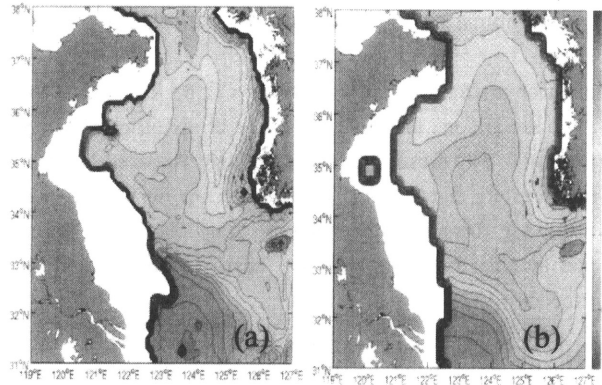


Fig 3. The temperature at 30 m in June: a) ExpQ.W_cT; b) Hirose (2011)

3.2 Lagrangian behavior

The Lagrangian behaviors of current in the southwestern Yellow Sea are studied by the trajectories of the artificial drifters. Table 1 shows the mean meridional displacement of the artificial drifter movements after 45 days in each experiment. Positive value means northward whereas negative one means southward. The artificial drifters, released at the

northeastern flank of Yangtze Bank, flow southeastward with high velocities following the tidal residual current (Fig 4a). The patterns of these trajectories closely resemble the structure of the Eulerian tidal residual current in this area. The mean meridional displacement

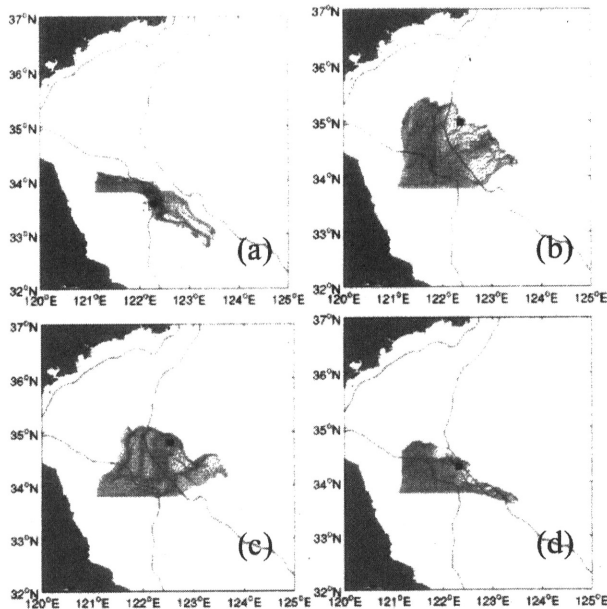


Fig 4. The trajectories of artificial drifters and the final gravity center of these drifters (square mark): (a) in ExpQ.T; (b) in ExpQ.W_c; (c) in ExpQ.W_cT and (d) the combination result of ExpQ.W_c and ExpQ.T.

of these artificial drifters is about -25.68 km (Table 1). As comparison, in ExpQ.W_c (only climatological wind forcing), all these artificial drifters released at the northeastern flank of Yangtze Bank flow northwestward following topographic isobaths (Fig 4b). The mean meridional displacement of these artificial drifters exceeds $+131.74$ km (Table 1).

Furthermore, in ExpQ.W_cT (both tidal and climatological wind forcing), the artificial drifters also move in the directions similar to those in ExpQ.W_c. The final gravity center of the artificial drifters flows northward about 112.76 km from the initial latitude (Fig 4c). Almost all these artificial drifters deployed at the northeastern flank of Yangtze Bank flow northward against the strong broad southeastward Eulerian tidal residual current over the sloping bottom around Yangtze Bank rather than follow it. This result corresponds with the northeastward ARGOS surface drifters released in the southwestern Yellow Sea in the summer season of 2009 (Li, 2010). The simple linear combination of ExpQ.W_c and ExpQ.T (Fig 4d) results in a mean meridional displacement of $+53.59$ km only (Table 1), which is much shorter than that of ExpQ.W_cT. The tidal

effect in ExpQ.W_cT is obviously weaker than what is expected from the linear combination result. Thus, the wind stress is the dominated forcing on the Lagrangian trajectories in the southwestern Yellow Sea.

Table 1. The list of experiments and the final mean meridional displacement in each experiment.

Experiment	Forcing	Bottom friction	Displacement (km)
ExpQ_T	only tidal forcing	quadratic bottom friction	-25.68
ExpQ_W _c	only climatological wind		$+131.74$
ExpQ_W _c T	both tidal and climatological wind		$+112.76$
Linear combination of ExpQ_W _c and ExpQ_T			$+53.59$
ExpL_T	only tidal forcing	linear bottom friction	
ExpL_W _c	only climatological wind		
ExpL_W _c T	both tidal and climatological wind		$+114.99$
Linear combination of ExpL_W _c and ExpL_T			$+102.71$

To further understand the dynamics of these Lagrangian phenomena, the effect of bottom friction has been examined utilizing the linear bottom friction scheme. ExpL.T, ExpL.W_c and ExpL.W_cT follow to the same conditions with ExpQ.T, ExpQ.W_c and ExpQ.W_cT, respectively, except that the linear bottom friction scheme.

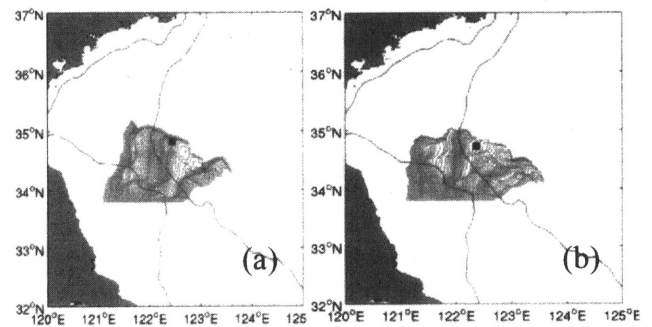


Fig 5. Same with Fig 4, but for: (a) ExpL.W_cT and (b) the combination result of ExpL.W_c and ExpL.T.

As shown in Fig 5a, ExpL.W_cT resembles ExpQ.W_cT after the calibration of the linear drag coefficients. The mean meridional displacement of these artificial drifters movement in ExpL.W_cT is about $+114.99$ km (Table 1). In contrast, the simple linear combination of ExpL.W_c and ExpL.T (Fig 5b) results in a mean meridional displacement of $+102.71$ km (Table 1), and it has relatively high similarity with ExpL.W_cT

contrast with nonlinear cases. These results indicate that, the influences of the tidal residual currents and wind stress on Lagrangian trajectories resembling closely follow the simple linear combination under the linear bottom friction scheme. Therefore, the nonlinearity of the bottom friction can lead to the weaker influence of the tidal residual currents on Lagrangian trajectories in the southwestern Yellow Sea. In other words, Lagrangian trajectory and Eulerian velocity could have different directions of movement at shallow coastal regions due to nonlinearity of the bottom friction.

As well known, bottom friction is an important sink of momentum and energy in the ocean. It plays a dynamic role in circulation, especially for the shallow area. The momentum fluxes at the bottom in POM are presented as following formula:

$$\rho \times (\langle wu(-1) \rangle, \langle wv(-1) \rangle) = -\rho C_D |\bar{u}| \bar{u} \quad (3)$$

where \bar{u} and C_D are same meanings with formula (1). While, in the light of the linear bottom friction parameterization approach as mentioned above (formula (2)), the momentum fluxes are:

$$\rho \times (\langle wu(-1) \rangle, \langle wv(-1) \rangle) = -\rho \Gamma_E \bar{u} \quad (4)$$

Formulas (3) and (4) have the similar expression based on the assuming $\Gamma_E = C_D U$, where ρ and U present the density of seawater and the typical friction velocity, respectively. ρ is equal to 1.025 kg/m^3 . U is independent of time and space, that is, it is a constant (0.5m/s) in the entire time and space, whereas, $|\bar{u}|$ is time and space dependent. Therefore, the momentum fluxes at the bottom in such simulations utilizing the linear Ekman parameterization will be acceptable only if U equivalent to the area-averaged value of $|\bar{u}|$. On the other hand, the spatial nonhomogeneity of the actual velocity field may lead to differences in some particular areas, which is the major limitation of linear bottom friction scheme. Consequently, the quadratic bottom friction scheme has higher accuracy comparing with the linear parameterization. The bottom momentum fluxes in each case are calculated on the basis of the formulas (3) and (4), moreover, the magnitudes of area-averaged are shown in Table 3. In accordance with previous description, the bottom momentum fluxes of ExpL.W_cT and ExpQ.W_cT are very similar as $12.3 \times 10^{-3} \text{ N/m}^2$ and $12.7 \times 10^{-3} \text{ N/m}^2$, respectively, which means the value of U in ExpL.W_cT is adequate. However, the bottom momentum flux in ExpL.T ($5.8 \times 10^{-3} \text{ N/m}^2$) is 28% weaker than that of ExpQ.T ($8.1 \times 10^{-3} \text{ N/m}^2$) in the shallow area, whereas, it is much enhanced in ExpL.W_c

($8.6 \times 10^{-3} \text{ N/m}^2$) in contrast to that of ExpQ.W_c ($1.7 \times 10^{-3} \text{ N/m}^2$). In this area, tidal currents are usually stronger than the typical friction velocity 0.5 m/s. Inversely, the wind-driven currents in this area are normally weaker than 0.5 m/s, which mean the bottom momentum fluxes of quadratic relation are weaker than that of linear relation. Thus, the higher bottom momentum fluxes in the simulation utilizing quadratic bottom friction scheme lead to the weaker tidal effect while stronger wind effect in the shallow area.

4. Conclusions

In this study, the POM model with an initial stratification was applied to study the influence of the tidal residual currents on Lagrangian trajectories during summer time in the southwestern Yellow Sea. Four kinds of tides (M_2 , S_2 , K_1 and O_1) and climatological wind stress forced the model from May to June. The simulated tidal harmonic constants agreed with the existing studies and observation well. The numerical model experiments also reproduced the patterns of Eulerian tidal residual currents in this region as shown in previous studies successfully.

The results of the model showed that the Lagrangian trajectories (Lagrangian velocities) were dominated by wind driven currents in the southwestern Yellow Sea. The influence of tidal residual currents on Lagrangian trajectories was weaker than that of southerly wind in summer time. Further analysis indicated that the quadratic bottom friction scheme is the crucial factor for the weaker influence of the tidal residual currents on Lagrangian trajectories in the southwestern Yellow Sea. This study demonstrates that Lagrangian trajectory and Eulerian velocity could have different directions of movement at shallow coastal regions due to nonlinearity of the bottom friction.

References

- 1) An, H. S., J. Oceanogr. Soc. 103-110(1977)33.
- 2) Beardsley, R. C., R. Limeburner, K. Kim, and J. Candela, Mer. 297-314(1992)30.
- 3) Chen, C., and R. C. Beardsley, J. Phys. Oceanogr. 2090-2110(1995)25.
- 4) Chen, C., R. C. Beardsley, and R. Limeburner, J. Phys. Oceanogr. 2111-2128(1995)25.
- 5) Choi, B. H., KORDI Report 80-02(1980), 72 pp.
- 6) Choi, B. H., In Ocean Hydrodynamics of the Japan and East China Seas, ed. by T. Ichiye, Elsevier, Amsterdam. 209-224(1984).
- 7) Choi, B. H., In Modeling Marine Systems, ed. by A.

- M. Davies. 167-185(1990).
- 8) Choi, B. H., K. O. Kim and H. M. Eum, Coastal Ocean Eng. 41-50(2002)14, (in Korean with English abstract).
 - 9) Fang, G., C. J. of Oceanology and Limnology. 1-16(1986)4.
 - 10) Gary, E., A. Bennett, and M. Foreman, J. Geophys. Res., 99,821-852(1994)24.
 - 11) Haney, R. L., J. Phys. Oceanogr. 610-619(1991)21.
 - 12) Hirose, N. J Oceanogr. (2011).
 - 13) Hu, D., M.Cui, Y. Li and T. Qu, Yellow Sea Research, 79-88 (1991)4.
 - 14) Hu, D.X., Oceanology of China Seas. 27-38 (1994)1.
 - 15) Hu, C. and M. X. He, Eos Trans. AGU. 302-303 (2008)89.
 - 16) Hu, C., Li. D, Chen C, Ge J, Muller-Karger FE, et al., J Geophys Res. 115(2010).
 - 17) Kang, S.K., Lee S.R. and Lei H.J., Continental shelf Research, 739-772(1998) 18(7).
 - 18) Kang, S.K., M. G. G. Foreman, H.-J, Lie, J.-H. Lee, J. Cherniawsky, and K.-D. Yum, J. Geophys. Res. 107(2002).
 - 19) Larsen, L. H., G. A. Cannon and B. H. Choi, Cont. Shelf Res. 77-103(1985)4.
 - 20) Lee, S.-H., and R. C. Beardsley, J. Geophys. Res. 679-701(1999)104.
 - 21) Li, Y., Doctor Thesis, IOCAS, 33-38(2010).
 - 22) Lie, H.-J., Prog. Oceanogr. 229-242 (1986)17.
 - 23) Liu, Z., Postdoctoral Report, IOCAS. 40-43(2006).
 - 24) Moon, J.-H., N. Hirose, and J.-H. Yoon, Journal of Geophysical Research. 114(2009).
 - 25) Naimie, C. E., C. A. Blain and D. R. Lynch, Continental shelf Research. 667-695 (2001)21.
 - 26) Nishida, H., Report of Hydrographic Researches. 55-70(1980)145.
 - 27) Ogura, S., Imperial Japanese Navy. 1-189(1933)7.
 - 28) Qiao, F., D. Ma, M. Zhu, R. Li, J. Zang, and H. Yu, Adv. Mar. Sci. 409-410(2008) 26(3).
 - 29) Shen, Y., Journal of Shandong College of Oceanology. 26-35(1980)10.
 - 30) Takahashi, S. and T. Yanagi, La Mer. 135-147(1995)33.
 - 31) Tang, Y., Zou E., Lie H., et al., Acta Oceanol.Sin. 1-16 (2000)22.
 - 32) Wan, Z., Qiao, F., Yuan, Y., Oceanologia ET Limnologia Sinica. 611-616 (1998)29.
 - 33) Xia, C., F. Qiao, Y. Yang, J. Ma, and Y. Yuan, J. Geophys. Res. (2006)111.
 - 34) Xu, D. F. Y. C. Yuan, Y. Liu, Ser. D. 117-126 (2002)46.
 - 35) Yanagi, T., Takahashi, S, Journal of Oceanography. 503-520. (1993)49.
 - 36) Yanagi, T. and K. Inoue, La mer. 153-165(1994)32.
 - 37) Yanagi, T., A. Morimoto and K. Ichikawa, J. Oceanogr. 303-310 (1997)53.
 - 38) Ye, A. and L. Mei, Oceanologia et Limnologia Sinica. 63-70(1995)26.
 - 39) Yuan, D., J. Zhu, C. Li, and D. Hu, Journal of Marine Systems. 134-149(2008)70.
 - 40) Zhao, B., G. Fang and D. Chao, Acta Oceanologica Sinica. 1-10(1994)16.